Structure-functional changes in eNAMPT at high concentrations mediate mouse and human beta- cell dysfunction in type 2 diabetes

Article

Accepted Version

TITLE: Structure-functional changes in eNAMPT at high concentrations mediate mouse and human beta-cell dysfunction in type 2 diabetes

AUTHORS: Sophie R. Sayers[1], Rebecca L. Beavil[2], Nicholas H.F. Fine[3,4], Guo Cai Huang[1], Pratik Choudhary[1] Kamila J. Pacholarz[5], Perdita E. Barran[5], Sam Butterworth[6], Charlotte E. Mills[7,8], J. Kennedy Cruickshank[7], Marta P. Silvestre[9], Sally D. Poppitt[9], Anne-Thea McGill[9,10], Gareth G. Lavery[3,4], David J. Hodson[3,4], Paul W. Caton[1,7]

[1]Department of Diabetes, School of Life Course Sciences, King's College London, UK

[2]Protein Production Facility, Randall Centre for Cell and Molecular Biophysics, King's College London, UK

[3]Institute of Metabolism and Systems Research (IMSR), and Centre of Membrane Proteins and Receptors (COMPARE), University of Birmingham, Birmingham, UK.

[4]Centre for Endocrinology, Diabetes and Metabolism, Birmingham Health Partners, Birmingham, UK.

[5]Michael Barber Centre for Collaborative Mass Spectrometry, Manchester Institute of Biotechnology, School of Chemistry, Manchester, UK

[6]Division of Pharmacy and Optometry, Faculty of Biology, Medicine and Health, University of Manchester, UK

[7]Department of Nutritional Sciences, School of Life Course Sciences, King's College London, UK

[8]Nutrition Research Group, University of Reading, UK

[9]Human Nutrition Unit, School of Biological Sciences, University of Auckland, New Zealand;

[10]School of Health & Human Sciences, Southern Cross University, Lismore, NSW 2480, Australia

The authors have declared that no conflict of interest exists.

Corresponding Author: Paul W. Caton, Diabetes Research Group, School of Life Course Sciences, King's College London, Hodgkin Building, Guy's Campus, London, SE1 1UL; TEL: +44 (0) 207 848 6111; Email, paul.w.caton@kcl.ac.uk. ORCID ID: 0000-0003-0902-0676

TWEET: Structure-functional changes in eNAMPT at high concentrations mediate mouse and human beta-cell dysfunction in type 2 diabetes @paulwcaton; @lifecourse_KCL @DRG_Kings

Word Count: 3999

Abstract

Aims/Hypothesis: Progressive decline in functional beta-cell mass is central to the development of type 2 diabetes. Elevated serum levels of extracellular nicotinamide phosphoribosyltransferase (eNAMPT) are associated with beta-cell failure in type 2 diabetes, and eNAMPT immuno-neutralization improves glucose tolerance in diabetic mice. Despite this, the effects of eNAMPT on functional beta-cell mass are poorly elucidated, with some studies having separately reported beta-cell protective effects of eNAMPT. eNAMPT exists in structurally and functionally distinct monomeric and dimeric forms. Dimerisation is essential for the NAD-biosynthetic capacity of NAMPT. Monomeric eNAMPT does not possess NAD-biosynthetic capacity, and may exert distinct NAD-independent effects. This study aimed to fully characterise the structure-functional effects of eNAMPT on pancreatic beta-cell functional mass and relate these to beta-cell failure in type 2 diabetes.

Methods: We generated recombinant wild-type and monomeric eNAMPT to explore the effects of eNAMPT on functional beta-cell mass in isolated mouse and human islets. Beta-cell function was determined by static and dynamic insulin secretion and intracellular calcium microfluorimetry. NAD-biosynthetic capacity of eNAMPT was assessed by colorimetric and fluorescent assays, and by native mass spectrometry. Islet cell number was determined by immunohistochemical staining for insulin, glucagon and somatostatin, with islet apoptosis determined by caspase 3/7 activity. Markers of inflammation and beta-cell identity were determined by qPCR. Total, monomeric and dimeric eNAMPT and NMN were evaluated by ELISA, western blot and fluorometric assay in non-diabetic, glucose intolerant and type 2 diabetes serum

Results: eNAMPT exerts bi-modal, concentration and structure-functional dependent effects on beta-cell functional mass. At low physiological concentrations (~1 ng/ml), as seen in non-diabetic serum, eNAMPT enhances beta-cell function through NAD-dependent mechanisms, consistent with eNAMPT being present as a dimer. However, as eNAMPT concentrations rise to ~5 ng/ml, as in type 2 diabetes, eNAMPT begins to adopt a monomeric form and mediates beta-cell dysfunction, reduced beta-cell identity and number, increased alpha-cell number and increased apoptosis, through NAD-independent pro-inflammatory mechanisms.

Conclusions/Interpretation: We have characterised a novel mechanism of beta-cell dysfunction in type 2 diabetes. At low physiological levels, eNAMPT exists in dimer form and maintains beta-cell function and identity through NAD-dependent mechanisms. However, as eNAMPT levels rise, as in type 2 diabetes, structure-function changes occur resulting in marked elevation of monomeric eNAMPT, which induces a diabetic phenotype in pancreatic islets. Strategies to selectively target monomeric eNAMPT could represent promising therapeutic strategies for treatment of type 2 diabetes.

Keywords: Beta-cell, Extracellular nicotinamide phosphoribosyltransferase (eNAMPT), Insulin secretion, Inflammation, NAD, Type 2 diabetes

Abbreviations:

$[Ca^{2+}]_{cyt:}$ Cytosolic calcium

eNAMPT**:** Extracellular nicotinamide phosphoribosyltransferase

FPG: Fasting plasma glucose

GSIS: Glucose stimulated insulin secretion

IFG: Impaired fasting glucose

iNAMPT: intra-cellular nicotinamide phosphoribosyltransferase

NMN: nicotinamide mononucleotide

NR: Nicotinamide riboside

PBEF: pre-B cell enhancing factor

SIRT: Sirtuin

Research in Context:

What is already known about the subject?

- Serum concentrations of extra-cellular nicotinamide phosphoribosyltransferase (eNAMPT) are elevated in type 2 diabetes.
- However previous studies have shown both deleterious and protective effects of eNAMPT on the pancreatic beta-cell.
- eNAMPT exists in monomer and dimer forms. Our previous studies have suggested that structure-functional relationships may mediate the diverse reported effects of eNAMPT.

What is the key question?

- What are the selective roles of monomeric and dimeric eNAMPT on pancreatic beta cell function and mass?

What are the new findings?

- Serum eNAMPT concentrations increase with progression from normoglycemia to type 2 diabetes. However, these increases are not associated with increasing eNAMPT NAD-biosynthetic activity, and are characterized by a marked increase in non-NAD biosynthetic monomeric eNAMPT and a relative decline in dimeric (NAD synthesizing) eNAMPT.

- At low, physiological levels eNAMPT is present solely in dimeric form and promotes beta-cell function through NAD-biosynthetic effects

- As levels of eNAMPT rise to pathophysiological levels (~5 ng/ml), as in type 2 diabetes, eNAMPT adopts monomeric form and induces beta-cell failure through NAD-independent effects

- Monomeric eNAMPT drives beta-cell failure in part through promoting islet inflammation.

How might this impact on clinical practice in the foreseeable future?

- Developing compounds to selectively target monomeric eNAMPT or stabilise eNAMPT in dimeric form could improve functional beta-cell mass and be used to treat type 2 diabetes, through both elevation of islet NAD levels and blocking of the pro-inflammatory NAD-independent effects of eNAMPT-monomer.

Introduction

Elucidating the underlying mechanisms responsible for progressive decline in functional beta-cell mass is essential for design of novel treatments for type 2 diabetes (1).

The protein nicotinamide phosphoribosyltransferase (NAMPT) exists in intra-cellular (iNAMPT) and extra-cellular (eNAMPT) forms. eNAMPT (visfatin/pre-B-cell enhancing factor) is a circulating protein with several reported functions (2-4). Similar to iNAMPT, eNAMPT may exert NAD-biosynthetic effects, whereby eNAMPT catalyses the conversion of nicotinamide to nicotinamide mononucleotide (NMN) in serum (5, 6). NMN may subsequently be transported into the cell (directly or via conversion into nicotinamide riboside), where it is converted into NAD by NMNATs1 – 3. However, this mechanism has been disputed and NAD-independent functions, including eNAMPT-mediated pro-inflammatory effects, are also reported (4, 7-9)

Serum eNAMPT levels are elevated in type 2 diabetes, in association with declining beta-cell function. Our in vivo studies indicate that eNAMPT may mediate type 2 diabetes pathophysiology (10-12). Contrasting studies report that eNAMPT and its reaction product NMN exert beta-cell protective effects via boosting of cellular NAD levels (6, 13-19).

A key, but frequently overlooked factor governing eNAMPT function is the presence of structurally and functionally distinct monomeric (~52 KDa) and dimeric (~104 KDa) eNAMPT. Dimerization is essential for NAD-biosynthetic capacity of eNAMPT (6, 20), and eNAMPT-dimer predominates in normal physiology [12,15]. eNAMPT-monomer does not possess NAD-biosynthetic capacity and may mediate NAD-independent pro-inflammatory effects. Our studies suggested a specific pathophysiological role for monomeric eNAMPT in diabetic mice (12). We hypothesised that in type 2 diabetes, eNAMPT-monomer is selective elevated, which exerts NAD-independent pro-inflammatory effects, and that this, combined with loss of eNAMPT NAD-biosynthetic capacity plays a key role in disease pathophysiology.

However, whether eNAMPT-monomer is elevated in T2D, and to what extent the structurally distinct forms of eNAMPT directly affect the pancreatic beta-cell are unknown. Previous studies, including our own, have examined NAD-boosting effects of NMN on beta-cell function (6, 13, 14), or have examined supraphysiological concentrations or acute effects of eNAMPT (21, 22), neither of which accurately mimic in vivo (patho)physiology. Of perhaps greater importance, the selective effects of monomeric and dimeric eNAMPT on beta-cell health have not been examined.

We used isolated mouse and human islets, and human type 2 diabetes serum, to specifically characterise effects of monomeric and dimeric eNAMPT on pancreatic beta-cell functional mass.

Materials and Methods

Animals

Eight-week-old male CD1 mice (28-33 g; Envigo, UK) were housed in 12-hour light/dark cycle temperature-controlled conditions with *ad libitum* access to standard mouse chow and water. Procedures were performed in accordance with U.K. Home Office regulations (Animal Scientific Procedures Act, 1986).

Human samples

Human serum was obtained from obese non-diabetic, IFG and type 2 diabetes individuals, as part of the BodyFatS&H study (University of Auckland, New Zealand) and separately from the VaSera trial(23) (St Thomas' Hospital, London). Study participants gave informed consent. Investigations were approved by NRES Committee- London Central (VaSera) and NREC, Auckland, New Zealand (BodyFatS&H). ESM Methods

Native Mass Spectrometry

Native Mass Spectrometry was conducted using Synapt G2S HDMS (Waters, Manchester, UK). ESM Methods.

eNAMPT protein generation

Recombinant wild-type eNAMPT (eNAMPT-WT) and mutant $SS^{199}/^{200}DD$ (eNAMPT-monomer) were produced in *E.Coli*. ESM Methods.

Pancreatic islet isolation and insulin secretion

Mouse islets were isolated between 9 – 10 am, (24). Human islets were isolated from heart-beating non-diabetic donors, with ethical approval, at the King's College Hospital Human Islet Isolation Unit (24). All isolated islets were incubated overnight (37°C, 5% CO_2) prior to treatments.

Static and dynamic glucose-stimulated insulin secretion

Static or dynamic insulin secretion was assessed in response to 2 or 20 mmol/l glucose exposure, as previously described [16]. Secreted insulin was measured by in-house I^{125} radioimmunoassay (25). ESM methods.

Endotoxin

Endotoxin concentrations were measured in recombinant eNAMPT preparations using the Pierce LAL Chromogenic Endotoxin Quantitation Kit (ThermoFisher Scientific).

In vitro islet immunostaining

Mouse islets were pelleted and fixed in 4% (vol/vol) buffered formalin. Sections (5 μmol/l) were incubated with anti-guinea pig insulin, anti-rabbit glucagon or anti-rabbit somatostatin (all Dako, 1:100) and DAPI (ThermoFisher). Secondary antibodies used were: AlexaFluor 488-labelled goat anti-mouse, AlexaFluor 594-labelled donkey anti-guinea-pig and AlexaFluor 488-labelled donkey anti-rabbit (1:200; all Jackson ImmunoResearch). Sections were mounted on glass slides and captured on a Nikon TE2000 fluorescent microscope and quantified using Image J.

Islet apoptosis

Mouse islets were treated with eNAMPT +/- cytokine cocktail (0.05 U/μl Il-1β, 1U/μl TNFα and IFNγ; 48 h). Apoptosis was determined by Caspase-Glo 3/7 luminescent assay (Promega, Southampton, UK).

Quantitative RT-PCR

Gene expression was determined by Sybr Green qRT-PCR using ΔΔCt methodology, normalised against GAPDH (Quantitech, UK). ESM Methods/ESM Table 1.

Intracellular calcium $[Ca^{2+}]_{cyt}$

Whole mouse islets, incubated in HEPES bicarbonate buffer (containing 2 – 20 mmol/L glucose), were loaded with Fura-2AM and imaged using a Nikon Ti-E microscope equipped with FuraLEDs (Cairn Research) (excitation = 340/385 nm, emission = 470-550 nm).

MIN6 cell culture

MIN6 cells (mycoplasma free) were cultured at 37°C in DMEM (25 mmol/l glucose; 2 mmol/l glutamine, 10% FBS, 100U/ml penicillin, 100μg/ml streptomycin) and treated with eNAMPT or NMN (48 h), prior to NAD and NMN measurements.

eNAMPT Immunoblotting

Serum eNAMPT-monomer and dimer were measured by immunoblotting, under non-reducing conditions, as previously described (26). ESM methods.

eNAMPT, NAD and NMN measurements

Total serum eNAMPT was measured by ELISA (Adipogen, Seoul, South Korea). MIN6 intracellular NAD and NMN levels were measured by NAD/NADH quantification kit, (Sigma-Aldrich, Poole, UK) and in-house fluorometric assay, respectively (27, 28). ESM methods.

Data Analysis

Data is expressed as mean ± SEM. Significance was tested using one or two-way ANOVA with Tukey's or Sidak's post-test, using GraphPad PRISM 7 software.

Results

Serum eNAMPT-monomer concentrations are elevated in type 2 diabetes and are positively correlated with increased HbA_{1c}

We first demonstrated that serum eNAMPT concentrations increased with progression of type 2 diabetes (Fig. 1a). In obese non-diabetic individuals, serum eNAMPT concentrations were 1.7 +/- 0.4 ng/ml; rising to 3.4 +/- 0.7 ng/ml in IFG, and 4.6 +/- 0.6 ng/ml in type 2 diabetes ($P<0.05$ vs. non-diabetic). These concentrations are similar to those observed in previous studies (29, 30)(31). Increasing eNAMPT concentrations strongly correlated ($R^2=0.3787$; $P<0.01$) with increasing HbA_{1c} (mmol/mol), indicating a role of eNAMPT in mediating poor glycaemic control (Fig. 1b). Next, we specifically measured serum eNAMPT-monomer and -dimer by immunoblotting under non-reducing conditions. eNAMPT-monomer was almost absent in ND serum, but increased markedly in T2D. Specifically, in ND serum, eNAMPT was 95.8% dimer and 4.2% monomer, but in T2D serum eNAMPT was 71% dimer and 29% monomer which translated into a concentration of 1.83 ng/ml eNAMPT-monomer in T2D serum (Fig 1c-e). Increasing eNAMPT concentrations did not correlate with serum NMN levels and NMN was not associated with HbA_{1c} (Fig. 1g-f). This suggests a selective pathophysiological role for eNAMPT-monomer in T2D. Neither eNAMPT nor NMN were correlated with BMI, age or serum insulin (ESM Fig. 1).

eNAMPT exerts bi-modal effects on beta-cell function in mouse and human pancreatic islets

Increased HbA_{1c} is indicative of poor glycaemic control and deteriorating beta-cell function. To assess the (patho)physiological effects of eNAMPT on beta-cells, we used serum eNAMPT concentrations (as detected in Fig 1A and (12)), and exposed isolated islets to physiological (1 ng/ml)) and pathophysiological (5 ng/ml) eNAMPT. To account for batch-to-batch differences between commercially available eNAMPT (8), we generated recombinant wild-type eNAMPT (eNAMPT-WT). To specifically examine eNAMPT-monomer, we mutated $Ser^{199/200}$ (key residues in the NAMPT binding interface (6, 20)) to aspartic acid. This generated a 52

KDa protein (eNAMPT-monomer), which neither dimerized correctly, as demonstrated by size-exclusion chromatography and native MS, nor synthesised cellular NMN and NAD (ESM Fig. 2a-e). Neither eNAMPT-WT nor eNAMPT-monomer contained notable endotoxin concentrations (ESM Fig. 2f)

eNAMPT-WT induced a bi-modal response. 1 ng/ml eNAMPT significantly enhanced static glucose-stimulated insulin secretion (GSIS) in mouse and human islets (24-48 h; Fig. 2a-b,e-f) and enhanced dynamic GSIS (48 h; $P<0.05$; Fig. 2h-i) and intra-cellular calcium levels ($[Ca^{2+}]_{cyt,}$) in mouse islets (Fig. 2l-m; AUC $P<0.01$). In contrast, neither 5 ng/ml eNAMPT-WT nor eNAMPT-monomer (0.1-5 ng/ml; 48 h) stimulated static or dynamic GSIS or increased intra-cellular calcium in mouse or human islets, with levels similar to or reduced compared untreated islets (Fig. 2a-m). A similar bi-modal insulin secretory response was observed following exposure to commercial eNAMPT (Adipogen, Seoul, South Korea) (ESM. 3a-c).

We also assessed effects of a combination of eNAMPT-WT and eNAMPT-monomer, which is more representative of normal (patho-)physiology. eNAMPT-WT (1 ng/ml) alone induced GSIS as expected; however, when eNAMPT-WT (1 ng/ml) was added in combination with eNAMPT-monomer, the insulin stimulatory effects of eNAMPT-WT were lost (Fig 2n).

Together this demonstrates that low, physiological eNAMPT enhances beta-cell function, but as eNAMPT rises to pathophysiological levels (~5 ng/ml), beneficial effects are lost and eNAMPT mediates beta-cell dysfunction. The effects of high concentrations of eNAMPT-WT are mimicked by non-dimerising eNAMPT-monomer, consistent with the notion that eNAMPT-WT adopts monomeric structure and function at higher concentrations.

Pathophysiological eNAMPT reduced beta-cell number and identity and increased alpha-cell number

Type 2 diabetes is characterised by reduced beta-cell mass, with loss of beta-cell identity, and increased apoptosis possible mechanisms. Consistent with the bi-modal insulin secretory response, mRNA levels of islet *INS2* and the essential beta-cell identity markers (32) *PDX1*, *NKX2.2* ($P<0.01$) and *NKX6.1* ($P<0.05$) (Fig. 3a-b) were increased by 1 ng/ml eNAMPT-WT but not 5 ng/ml eNAMPT-WT, nor 1 ng/ml eNAMPT-monomer (48h; Fig. 3a-c). 5 ng/ml eNAMPT-WT also enhanced cytokine-mediated islet apoptosis, (caspase3/7 activity) ($p<0.001$, Fig. 3d), as well as significantly reducing insulin$^+$ cells and increasing glucagon$^+$ ($P<0.05$) and somatostatin$^+$ cells denoting decreased beta-cell and increased alpha- and delta-cell number, respectively (Fig. 3e–k; ESM Fig 4).

eNAMPT impairs beta-cell function via pro-inflammatory mechanisms

Pro-inflammatory effects of eNAMPT are reported, although to date, not in type 2 diabetes. eNAMPT-WT at 5 ng/ml, but not 1 ng/ml (48 h) increased mouse islet *Il1B* ($P<0.05$) and *CCL2* ($P<0.001$) gene expression (Fig. 4a). Similarly, eNAMPT-monomer (1 ng/ml; 48 h) increased *Il1B* and *CCL2* gene expression in mouse and human islets ($P<0.05$) (Fig. 4b). Inflammatory pathway inhibitors (Tocris Biosciences, Abingdon UK) demonstrated that inhibition of STAT3 (using NCS74859) and P38-MAPK (using SB203580), but not of NFκB (using BAY 11-7082) or JNK (using SP600125), blocked the inhibitory effects of eNAMPT on GSIS (Fig. 4c).

Therefore, pathophysiological concentrations of eNAMPT-WT and eNAMPT-monomer induce beta-cell dysfunction, in part through promotion of STAT3 and P38-mediated islet inflammation.

Structure-function changes mediate bi-modal effects of eNAMPT-WT

Since the effects of eNAMPT-monomer were mimicked by 5 ng/ml, but not 1 ng/ml eNAMPT-WT, we hypothesised that high concentrations of eNAMPT-WT (5 ng/ml) would be associated with reduced NAD biosynthetic capacity (compared to 1 ng/ml) indicative of reduced eNAMPT-dimer and increased eNAMPT-monomer levels.

In support of this, 1 ng/ml eNAMPT-WT (48 h) increased cellular NMN and NAD, 30% ($P<0.05$) and 20% above basal levels, respectively, in MIN6 cells. These changes were mimicked by NMN treatment (100 μmol/l; 48 h; Sigma-Aldrich, Poole, UK) (Fig 5a-d). NMN also mimicked functional effects of 1 ng/ml eNAMPT-WT, significantly increasing levels of GSIS and *INS2, NKX2.2* and *PDX1* mRNA (Fig. 5e–f). In contrast, and similar to effects of eNAMPT-monomer, 5 ng/ml eNAMPT-WT did not increase cellular NMN nor NAD (Fig. 5a-d; ESM Fig. 2d-e). Furthermore, AMCP-mediated inhibition of CD73 (a protein involved in cellular NMN uptake) (33-36)(37) inhibited the insulin secretory effects of 1ng/ml eNAMPT-WT ($P<0.05$), but had no effects on the inhibitory actions of 5 ng/ml eNAMPT-WT on GSIS (Fig. 5g). Thus, 1 ng/ml eNAMPT induces NAD biosynthesis and requires islet NMN uptake to exert functional effects. In contrast, effects of 5 ng/ml eNAMPT were unaffected by inhibition of NMN uptake, suggesting an NAD-independent pathway.

This data provides evidence that the bi-modal effects of eNAMPT-WT are related to loss of NAD-biosynthetic capacity of eNAMPT at higher concentrations.

Discussion

This study demonstrates that eNAMPT exerts bi-modal, concentration and structure-function dependent effects on pancreatic beta-cell functional mass, and provides clarification of previous contradictory eNAMPT studies.

Low, physiological levels of eNAMPT (1 ng/ml) enhance beta-cell health through NAD-dependent mechanisms. Since islets are continually exposed to low eNAMPT concentrations in healthy non-diabetic individuals, this indicates a role for low eNAMPT concentrations in maintaining beta-cell health. Beta-cell identity genes were increased at 1 ng/ml eNAMPT, highlighting the potential importance of physiological eNAMPT in maintaining beta-cells in fully differentiated state, consistent with studies showing beta-cell de-differentiation following 3-day culture in the absence of circulating factors, including eNAMPT/NMN (41). The effects of 1 ng/ml eNAMPT are mediated via NAD-biosynthesis, suggesting eNAMPT exists in dimeric form at lower concentrations. This is consistent with our observations in non-diabetic human and mouse serum which show eNAMPT-dimer as the predominant structural form at low physiological concentrations (12). Whether eNAMPT can exert NAD-biosynthesis within extra-cellular space remains controversial. Whilst RPMI media contains sufficient nicotinamide to support eNAMPT enzymatic activity, we were unable to detect eNAMPT within spent islet media after eNAMPT incubation, suggesting that at least some eNAMPT-dimer is taken up into the islet/beta-cell, after which NMN synthesis occurs intra-cellularly.

Mechanistically, eNAMPT-mediated NAD synthesis may improve beta-cell health through activation of NAD-dependent sirtuins or via actions of NAD metabolites cADPR and NAADP which reportedly induce intra-cellular calcium mobilisation (13, 14, 16, 19).

Conversely, as eNAMPT concentrations rise to pathophysiological levels, as in type 2 diabetes, eNAMPT induces islet inflammation, and initiates beta-cell dysfunction, beta-cell death and reduced beta-cell mass and identity. The mechanisms driving reduced beta-cell number and identity are unclear. We have demonstrated that high concentrations of eNAMPT enhance beta-cell apoptosis, however beta- to alpha-cell trans-differentiation or beta-cell de-differentiation, may also play a role, and further studies are required to identify the precise mechanisms.

eNAMPT exerts beta-cell dysfunction through NAD-independent mechanisms, suggesting a switch toward monomeric eNAMPT at higher concentrations. This is consistent with observations that eNAMPT-monomer was present at 1-2 ng/ml in T2D serum, but almost absent in non-diabetic serum, and also consistent with our observations that increasing serum eNAMPT did not correlate with increasing serum NMN.

Whilst elevated eNAMPT strongly correlated with increased HbA_{1c}, we did not observe notable correlations between eNAMPT and BMI, and only a weak correlation between eNAMPT and serum insulin. We hypothesise that as glucose rises during glucose intolerance, secretion of eNAMPT-dimer increases, which promotes islet compensation. However, as eNAMPT levels continue to rise in response to elevated glucose, eNAMPT-dimer begins to break apart into constituent eNAMPT-monomers, which then drive beta-cell failure. Thus, eNAMPT

increases strongly correlate with increases in blood glucose and HbA_{1c}, and do not necessarily precede hyperglycaemia. Precisely why eNAMPT preferentially exists as a monomer at high levels remains unclear but may relate to ligand-induced dimerization, whereby eNAMPT is stabilised and maintained in dimer form by the presence of an endogenous ligand. We hypothesise that insufficient concentrations of the putative ligand at higher eNAMPT concentrations lead to break up the dimer into constitutive monomers.

Mechanistically, eNAMPT promoted islet inflammation and beta-cell failure, through P38-MAPK and STAT3 pathways. Similar eNAMPT effects are reported in macrophages, monocytes and islets of HFD mice (7, 9, 12, 38). Upstream, these effects may be receptor-mediated, with eNAMPT reported to function via TLR4 (39), CCR5 (40), IGF and IR (8) signalling, although these remain unconfirmed. Separately, the deleterious effects of eNAMPT-monomer may also reflect decreased eNAMPT-dimer mediated NAD synthesis, occurring separately from direct effects of eNAMPT-monomer.

Together, our results characterise structure-functional relationships as being of crucial importance to the effects of eNAMPT on beta-cell health. Moreover, we demonstrate a novel mechanism of beta-cell dysfunction in type 2 diabetes. Strategies to block actions of eNAMPT-monomer by promoting dimerization or stabilizing eNAMPT in dimer form could represent promising therapeutic approaches for treatment of diabetes.

Author Contributions

SRS, GCH, PC, RLB, NHFF, KJP, PEB, SB, DJH, GGL and PWC designed and conducted research, analysed data and reviewed and approved the final manuscript; ATM, MPS and SDP designed, conducted and analysed the BodyFatS&H study and reviewed and approved the final manuscript; CEM and JKC designed, conducted and analysed the VaSera study and reviewed and approved the final manuscript. SRS and PWC wrote the paper. PWC is the guarantor of this work. Data are available on request from the authors

Acknowledgements

We thank Prof Jun-ichi Miyazaki, (Osaka University, Osaka, Japan) for provision and consent to use MIN6 cells. Imaging was conducted in the Nikon Imaging Centre at King's College London.

Funding

P.W.C and SRS were supported by Diabetes UK project grants (15/0005154; 18/0005865), King's Health Partners Challenge Fund (funded via MRC Confidence-in-concept), Society for Endocrinology Early Career Grant and EFSD/Lilly Fellowship. D.J.H. was supported by a Diabetes UK R.D. Lawrence (12/0004431) Fellowship, and MRC (MR/N00275X/1) and Diabetes UK (17/0005681) Project Grants. This project has received

funding from the European Research Council (ERC) under the European Union's Horizon 2020 research and innovation programme (Starting Grant 715884 to D.J.H.), and New Zealand Health Research Council (HRC) programme grant (190/C; SDP and A-TM). MFS was supported by University of Auckland FRDF fellowship and HRC project grant (14/191). GGL was supported by a Wellcome Trust Senior Fellowship. The VaSera trial was supported by FUKUDA Denshi Japan. The Body Fat, Surgery and Hormone study (BodyFatS&H) conducted at the University of Auckland, New Zealand (NTX/08/10/103). The VaSera trial(23), conducted at St Thomas' Hospital, London (ISRCTN25003627; NRES Committee- London Central, 21/12/2012, ref: 12/LO/1850). The study funders were not involved in the design of the study; the collection, analysis, and interpretation of data; writing the report; or the decision to submit the report for publication

Duality of interest

The authors declare that there is no duality of interest associated with this manuscript.

References

1. DeFronzo RA, Abdul-Ghani MA. Preservation of beta-cell function: the key to diabetes prevention. The Journal of clinical endocrinology and metabolism. 2011;96(8):2354-66.
2. Imai S. Nicotinamide phosphoribosyltransferase (Nampt): a link between NAD biology, metabolism, and diseases. Curr Pharm Des. 2009;15(1):20-8.
3. Imai S, Yoshino J. The importance of NAMPT/NAD/SIRT1 in the systemic regulation of metabolism and ageing. Diabetes, obesity & metabolism. 2013;15 Suppl 3:26-33.
4. Samal B, Sun Y, Stearns G, Xie C, Suggs S, McNiece I. Cloning and characterization of the cDNA encoding a novel human pre-B-cell colony-enhancing factor. Mol Cell Biol. 1994;14(2):1431-7.
5. Rongvaux A, Shea RJ, Mulks MH et al. Pre-B-cell colony-enhancing factor, whose expression is up-regulated in activated lymphocytes, is a nicotinamide phosphoribosyltransferase, a cytosolic enzyme involved in NAD biosynthesis. Eur J Immunol. 2002;32(11):3225-34.
6. Revollo JR, Korner A, Mills KF et al. Nampt/PBEF/Visfatin regulates insulin secretion in beta cells as a systemic NAD biosynthetic enzyme. Cell Metab. 2007;6(5):363-75.
7. Li Y, Zhang Y, Dorweiler B, Cui D, Wang T, Woo CW, et al. Extracellular Nampt promotes macrophage survival via a nonenzymatic interleukin-6/STAT3 signaling mechanism. J Biol Chem. 2008;283(50):34833-43.
8. Fukuhara A, Matsuda M, Nishizawa M et al. Visfatin: a protein secreted by visceral fat that mimics the effects of insulin. Science. 2005;307(5708):426-30.
9. Moschen AR, Kaser A, Enrich B et al. Visfatin, an adipocytokine with proinflammatory and immunomodulating properties. J Immunol. 2007;178(3):1748-58.
10. Lopez-Bermejo A, Chico-Julia B, Fernandez-Balsells M et al. Serum visfatin increases with progressive beta-cell deterioration. Diabetes. 2006;55(10):2871-5.
11. Chang YH, Chang DM, Lin KC, Shin SJ, Lee YJ. Visfatin in overweight/obesity, type 2 diabetes mellitus, insulin resistance, metabolic syndrome and cardiovascular diseases: a meta-analysis and systemic review. Diabetes Metab Res Rev. 2011;27(6):515-27.
12. Kieswich J, Sayers SR, Silvestre MF, Harwood SM, Yaqoob MM, Caton PW. Monomeric eNAMPT in the development of experimental diabetes in mice: a potential target for type 2 diabetes treatment. Diabetologia. 2016;59(11):2477-86.
13. Caton PW, Kieswich J, Yaqoob MM, Holness MJ, Sugden MC. Nicotinamide mononucleotide protects against pro-inflammatory cytokine-mediated impairment of mouse islet function. Diabetologia. 2011;54(12):3083-92.

14. Caton PW, Richardson SJ, Kieswich J et al. Sirtuin 3 regulates mouse pancreatic beta cell function and is suppressed in pancreatic islets isolated from human type 2 diabetic patients. Diabetologia. 2013;56(5):1068-77.
15. Yoon MJ, Yoshida M, Johnson S et al. SIRT1-Mediated eNAMPT Secretion from Adipose Tissue Regulates Hypothalamic NAD+ and Function in Mice. Cell metabolism. 2015;21(5):706-17.
16. Yoshino J, Mills KF, Yoon MJ, Imai S. Nicotinamide mononucleotide, a key NAD(+) intermediate, treats the pathophysiology of diet- and age-induced diabetes in mice. Cell Metab. 2011;14(4):528-36.
17. Kim DS, Kang S, Moon NR, Park S. Central visfatin potentiates glucose-stimulated insulin secretion and beta-cell mass without increasing serum visfatin levels in diabetic rats. Cytokine. 2014;65(2):159-66.
18. Spinnler R, Gorski T, Stolz K et al. The adipocytokine Nampt and its product NMN have no effect on beta-cell survival but potentiate glucose stimulated insulin secretion. PLoS One. 2013;8(1):e54106.
19. Ramsey KM, Mills KF, Satoh A, Imai S. Age-associated loss of Sirt1-mediated enhancement of glucose-stimulated insulin secretion in beta cell-specific Sirt1-overexpressing (BESTO) mice. Aging cell. 2008;7(1):78-88.
20. Wang T, Zhang X, Bheda P, Revollo JR, Imai S, Wolberger C. Structure of Nampt/PBEF/visfatin, a mammalian NAD+ biosynthetic enzyme. Nat Struct Mol Biol. 2006;13(7):661-2.
21. Xiang RL, Mei M, Su YC, Li L, Wang JY, Wu LL. Visfatin Protects Rat Pancreatic beta-cells against IFN-gamma-Induced Apoptosis through AMPK and ERK1/2 Signaling Pathways. Biomed Environ Sci. 2015;28(3):169-77.
22. Brown JE, Onyango DJ, Ramanjaneya M et al. Visfatin regulates insulin secretion, insulin receptor signalling and mRNA expression of diabetes-related genes in mouse pancreatic beta-cells. Journal of molecular endocrinology. 2010;44(3):171-8.
23. Mills CE, Govoni V, Faconti L et al. Reducing Arterial Stiffness Independently of Blood Pressure: The VaSera Trial. Journal of the American College of Cardiology. 2017;70(13):1683-4.
24. Huang GC, Zhao M, Jones P et al. The development of new density gradient media for purifying human islets and islet-quality assessments. Transplantation. 2004;77(1):143-5.
25. Jones PM, Salmon DM, Howell SL. Protein phosphorylation in electrically permeabilized islets of Langerhans. Effects of Ca2+, cyclic AMP, a phorbol ester and noradrenaline. The Biochemical journal. 1988;254(2):397-403.
26. Caton PW, Nayuni NK, Kieswich J, Khan NQ, Yaqoob MM, Corder R. Metformin suppresses hepatic gluconeogenesis through induction of SIRT1 and GCN5. The Journal of endocrinology. 2010;205(1):97-106.
27. Formentini L, Moroni F, Chiarugi A. Detection and pharmacological modulation of nicotinamide mononucleotide (NMN) in vitro and in vivo. Biochemical pharmacology. 2009;77(10):1612-20.
28. Zhang RY, Qin Y, Lv XQ et al. A fluorometric assay for high-throughput screening targeting nicotinamide phosphoribosyltransferase. Analytical biochemistry. 2011;412(1):18-25.
29. Retnakaran R, Youn BS, Liu Y et al. Correlation of circulating full-length visfatin (PBEF/NAMPT) with metabolic parameters in subjects with and without diabetes: a cross-sectional study. Clin Endocrinol (Oxf). 2008;69(6):885-93.
30. Flehmig G, Scholz M, Kloting N et al. Identification of adipokine clusters related to parameters of fat mass, insulin sensitivity and inflammation. PLoS One. 2014;9(6):e99785.
31. Esteghamati A, Alamdari A, Zandieh A et al. Serum visfatin is associated with type 2 diabetes mellitus independent of insulin resistance and obesity. Diabetes Res Clin Pract. 2011;91(2):154-8.
32. Marchetti P, Bugliani M, De Tata V, Suleiman M, Marselli L. Pancreatic Beta Cell Identity in Humans and the Role of Type 2 Diabetes. Frontiers in cell and developmental biology. 2017;5:55.
33. Fletcher RS, Ratajczak J, Doig CL et al. Nicotinamide riboside kinases display redundancy in mediating nicotinamide mononucleotide and nicotinamide riboside metabolism in skeletal muscle cells. Molecular metabolism. 2017;6(8):819-32.
34. Ratajczak J, Joffraud M, Trammell SA et al. NRK1 controls nicotinamide mononucleotide and nicotinamide riboside metabolism in mammalian cells. Nature communications. 2016;7:13103.

35. Nikiforov A, Dolle C, Niere M, Ziegler M. Pathways and subcellular compartmentation of NAD biosynthesis in human cells: from entry of extracellular precursors to mitochondrial NAD generation. The Journal of biological chemistry. 2011;286(24):21767-78.
36. Garavaglia S, Bruzzone S, Cassani C et al. The high-resolution crystal structure of periplasmic Haemophilus influenzae NAD nucleotidase reveals a novel enzymatic function of human CD73 related to NAD metabolism. The Biochemical journal. 2012;441(1):131-41.
37. Yegutkin GG, Marttila-Ichihara F, Karikoski M et al. Altered purinergic signaling in CD73-deficient mice inhibits tumor progression. European journal of immunology. 2011;41(5):1231-41.
38. Matsuda T, Omori K, Vuong T et al. Inhibition of p38 pathway suppresses human islet production of pro-inflammatory cytokines and improves islet graft function. Am J Transplant. 2005;5(3):484-93.
39. Camp SM, Ceco E, Evenoski CL et al. Unique Toll-Like Receptor 4 Activation by NAMPT/PBEF Induces NFkappaB Signaling and Inflammatory Lung Injury. Scientific reports. 2015;5:13135.
40. Van den Bergh R, Morin S, Sass HJet al. Monocytes contribute to differential immune pressure on R5 versus X4 HIV through the adipocytokine visfatin/NAMPT. PloS one. 2012;7(4):e35074.

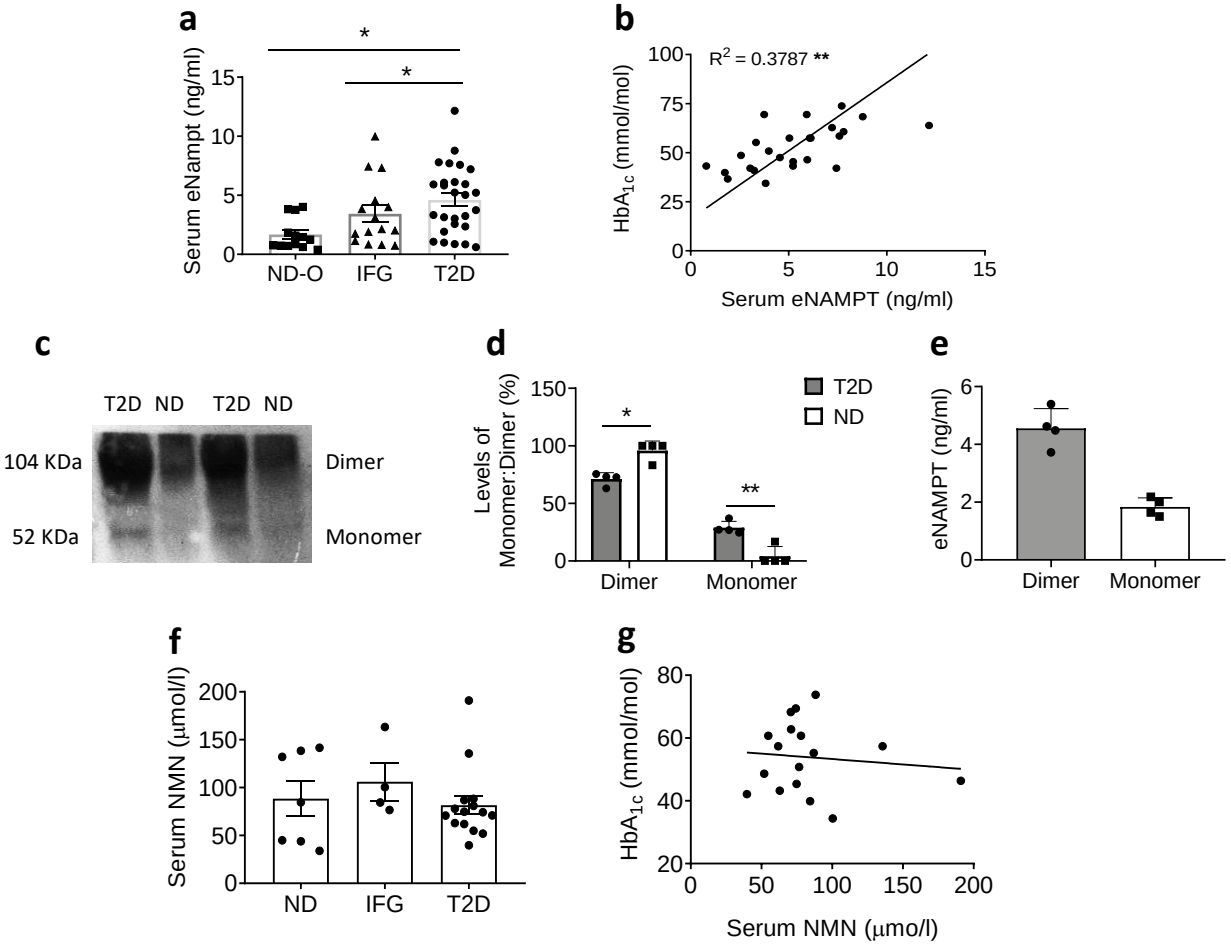

Figure 1: Serum eNAMPT levels are increased in type 2 diabetes and are associated with increased HbA_{1c}. Serum was collected from non-diabetic, IFG and type 2 diabetic individuals and eNAMPT was measured by ELISA**. (a)** Serum eNAMPT (data generated from BodyFatS&H and VaSera trial samples); **(b)** Serum eNAMPT vs. HbA_{1c} (mmol/mol) (data generated from VaSera trial only). **(c)** Western blot of serum eNAMPT monomer and dimer; **(d)** Percentage ratio of eNAMPT monomer and dimer in ND and T2D serum; **(e)** Calculated concentration of eNAMPT-monomer and dimer in T2D serum; **(f)** Serum NMN; **(g)** Serum NMN vs HbA_{1c} (mmol/mol) (data generated from VaSera trial only); ND = obese non-diabetic (BMI>30 kg/m^2; FPG = <5.6 mmol/L) (n=13); IFG (impaired fasting glucose; FPG 5.6 – 6.9 mmol/L; BMI>30 kg/m^2) (n=15); type 2 diabetes (FPG≥7.0 mmol/L; BMI>30 kg/m^2) (n=27). N is equal to 1 individual. N values differ for NMN measurements due to limited sample availability for some samples. Data are expressed as means ± SEM. * P<0.05; **P<0.01, calculated by 1-way ANOVA with Tukey's post-test, or Pearson correlation. Western blots are representative of 3 separate blots. To ensure equivalent loading of each gel lane, serum protein was equalized to 10 μg and an equal volume (30 μl) was added to each well.

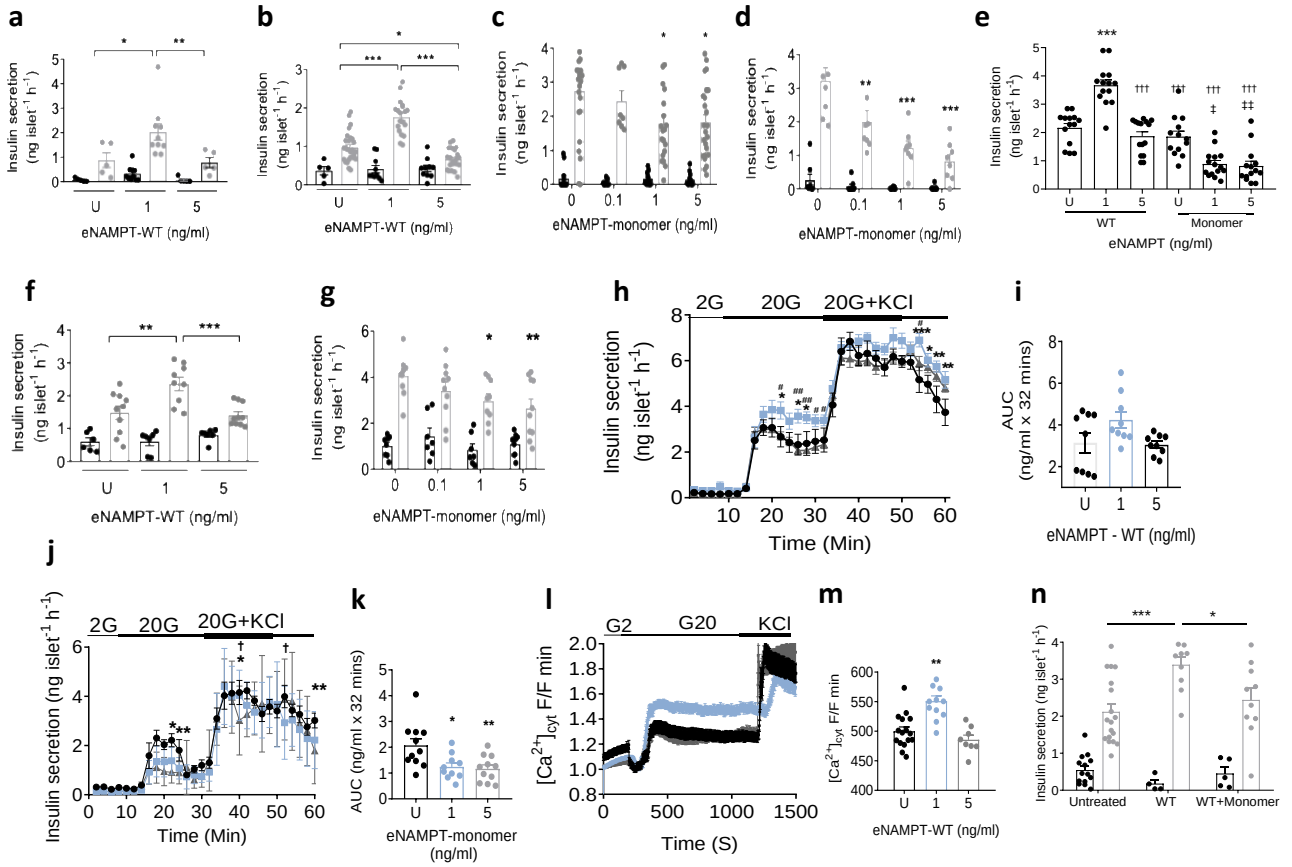

Figure 2: Glucose-stimulated insulin secretion has a bi-modal response to eNAMPT. (a – d) Static insulin secretion in response to basal (2 mmol/l) or 20 mmol/l glucose was assessed in isolated mouse islets incubated with 1 – 5 ng/ml eNAMPT-WT for **(a)** 24 and **(b)** 48 h or with 0.1 – 5 ng/ml eNAMPT-monomer for **(c)** 24 h and **(d)** 48 h; **(e)** Static insulin secretion in response to 20mM glucose was assessed in isolated mouse islets incubated with 1 – 5 ng/ml eNAMPT-WT and eNAMPT-monomer**. (f – g)** Static insulin secretion in response to basal (2 mmol/l) or 20 mmol/l glucose was assessed in isolated human islets incubated with 1 – 5 ng/ml eNAMPT-WT or 0.1 – 5 ng/ml eNAMPT-monomer for 48 h. For static GSIS, n=5 – 28, where an n of 1 = 5 islets/incubation tube, repeated 8 – 10 times. **(h – k)** Dynamic insulin secretion was assessed in isolated mouse islets incubated with **(h-i)** 1 – 5 ng/ml eNAMPT-WT or with **(j-k)** 1 – 5 ng/ml eNAMPT-monomer for 48 hours by perifusion with 2 mmol/l or 20 mmol/l glucose and 20 mmol/l KCl. For perifusion, n= 9-12, where an n of 1 equals one perifusion of 160 islets isolated from 4 – 6 mice); **(l – m)** Glucose-stimulated $[Ca^{2+}]_{cyt}$ was measured in isolated mouse islets treated with 1 – 5ng/ml eNAMPT-WT for 48 hours, *(n*= 3 mice/treatment, 9-16 islets/treatment). **(n)** Static insulin secretion in response to basal (2 mmol/l) or 20 mmol/l glucose was assessed in isolated mouse islets incubated with a combination of 1 ng/ml eNAMPT-WT and 1 ng/ml eNAMPT-monomer for 48 hours *(n*= 4-19). **(a – g,n)** grey bars = 2 mmol/l glucose; black bars = 20 mmol/l glucose; **(h,j, l)** black = untreated; blue = 1ng/ml eNAMPT-WT; grey = 5 ng/ml eNAMPT-WT; **(k,m)** black lines = untreated; blue lines = 1 ng/ml eNAMPT-monomer; grey bars = 5 ng/ml eNAMPT-monomer. Data are expressed as means

± SEM, **(a-d; f-n)** *P<0.05 (vs. 1 ng/ml eNAMPT-WT), **P<0.01 (vs. 1 ng/ml eNAMPT-WT), ***P<0.001, by 1- and 2-way ANOVA. **(e)** ***P<0.001 vs untreated (WT); ††† P<0.001 vs 1 ng/ml eNAMPT-WT by 1- way ANOVA; ‡ P<0.05, ‡‡ P<0.01 vs untreated (monomer)

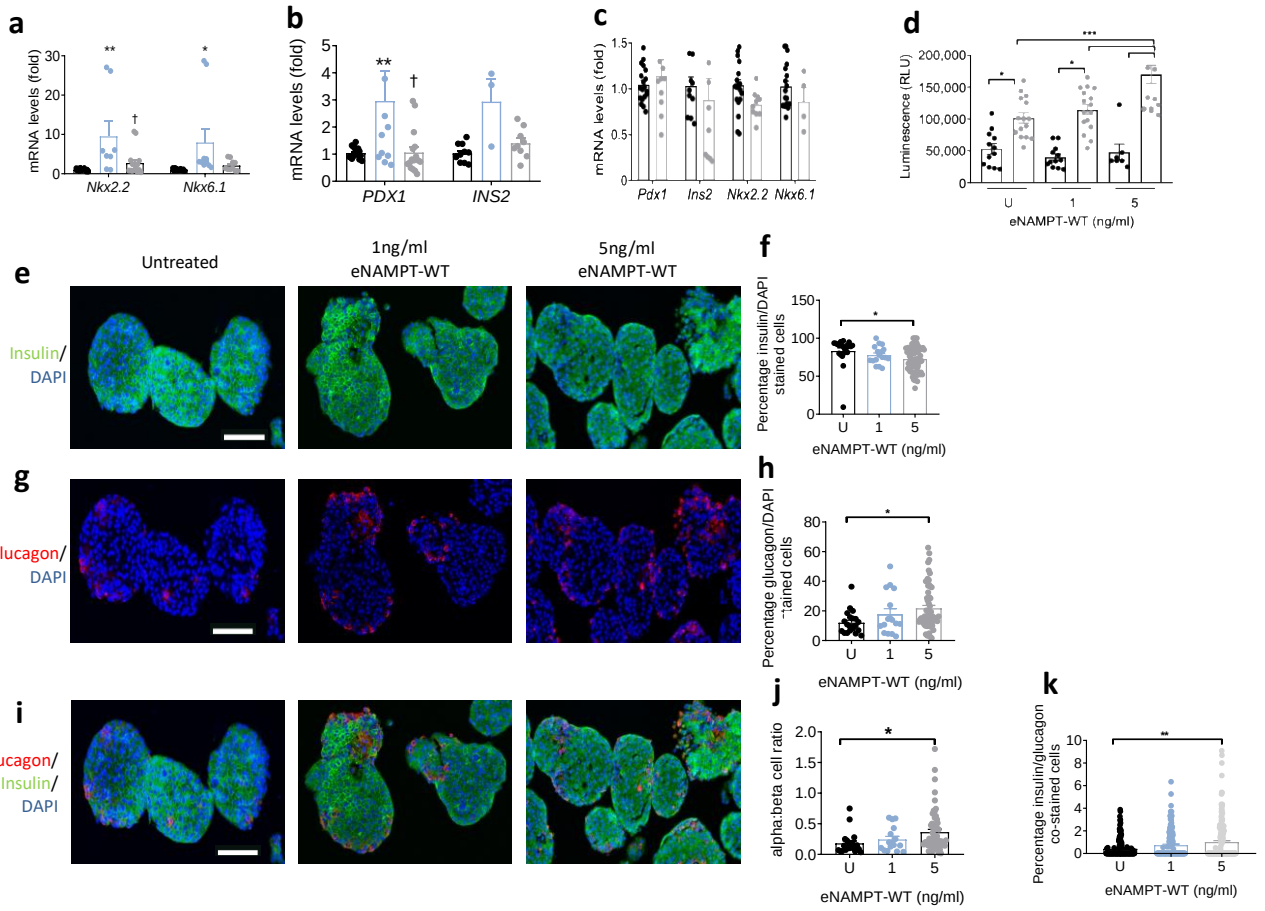

Figure 3: Monomeric eNAMPT mediates reductions in beta-cell identity and number (a – c) Gene expression of *Nkx2.2*, *Nkx6.1*, *Pdx1*, *INS2* was measured in mouse islets were treated with **(a – b)** 1 – 5 ng/ml eNAMPT-WT or **(c)** 1 ng/ml eNAMPT-monomer for 48 h; **(d) Apoptosis:** Caspase-3/7 activity was measured in islets treated with eNAMPT-WT with/without a cocktail of cytokines (TNFα, IFNγ and IL1β) (*n*= 7-16); **(e – k)** Mouse islets were treated with 1 – 5 ng/ml eNAMPT-WT for 48 h **(e)** Double immunofluorescence images of islets stained for insulin (green) and DAPI (blue) **(f)** % DAPI/insulin positive stained cells *(n*=3, where n of 1 = 200 – 300 islets from one mouse); **(g)** Double immunofluorescence images of islets stained for glucagon (red) and DAPI (blue) **(h)** % DAPI/glucagon positive stained cells *(n*=3); **(i)** Immunofluorescence images of islets stained for insulin (green), glucagon (red) and DAPI (blue) **(j)** % DAPI/glucagon:% DAPI/insulin stained cells *(n*=3); **(k)** % GLU^+/INS^+ bi-hormonal cells **(a, b)** black = untreated; blue = 1ng/ml eNAMPT-WT; grey = 5 ng/ml; **(c)** black bars = untreated; grey bars = 1 ng/ml eNAMPT-monomer; **(d)** black bars = no cytokines; grey bars = with cytokines. eNAMPT-WT Data are expressed as means ± SEM, *P<0.05, #P<0.05 (vs. 1 ng/ml eNAMPT-WT), **P<0.01, ***P<0.001, by 1- and 2-way ANOVA.

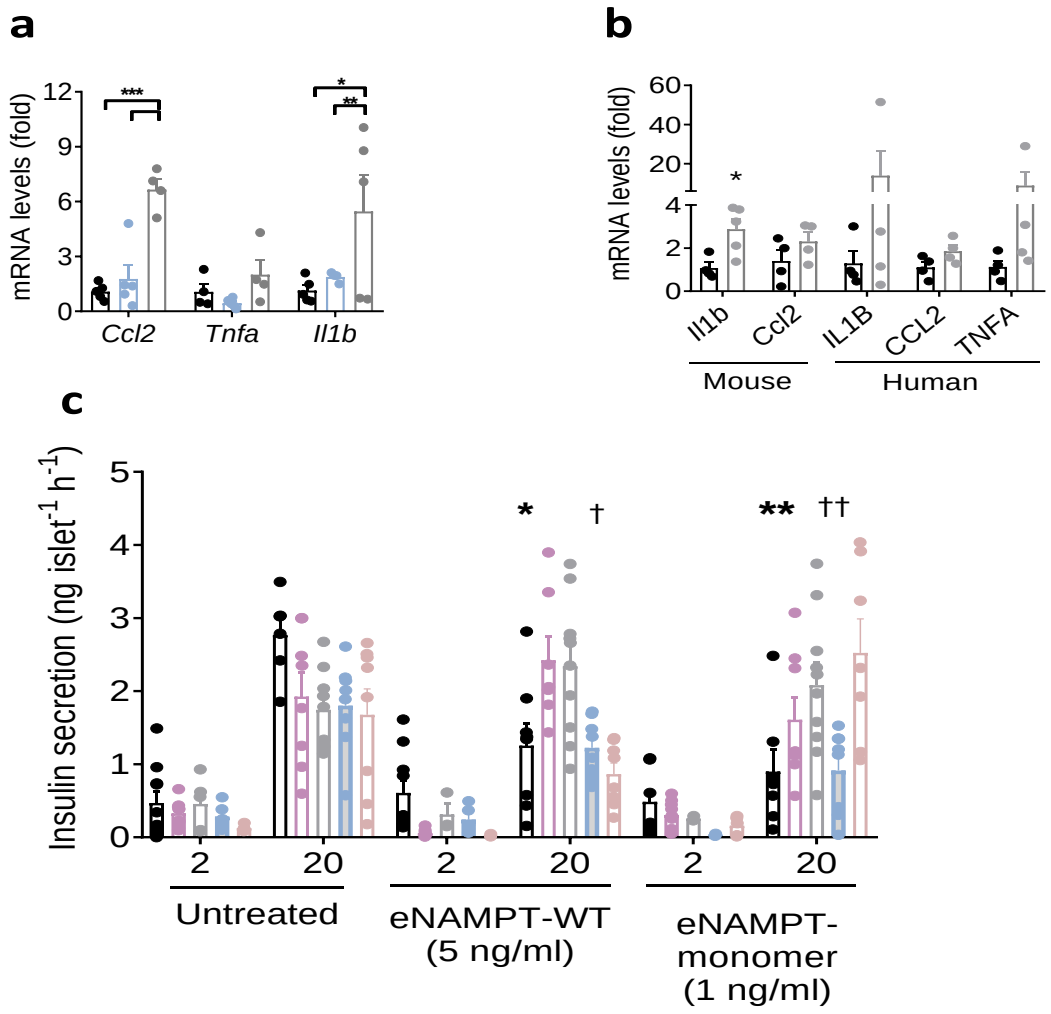

Figure 4: Monomeric eNAMPT impairs GSIS via pro-inflammatory mechanisms (a) Gene Expression of *CCL2*, *TNFA* and *IL1B* in mouse islets after treatment with eNAMPT-WT *(n*=4-5). **(b)** Gene Expression of *CCL2*, *TNFA* and *IL1B* in mouse and human islets after treatment with eNAMPT-monomer (*n*=4-5). **(c)** Mouse islets were treated with 5ng/ml eNAMPT-WT or 1ng/ml eNAMPT-monomer in combination with inhibitors of P38 (SB203580; 1 μmol/l), STAT3 (SB203580; 50 μmol/l), JNK (SP600125; 50 μmol/l) or NFκB (BAY 11-7082; 1 μmol/l) for 48 h and insulin secretion was measured after static incubation in 2 mmol/l (not shown) or 20 mmol/l glucose (*n* = 8-10). Data are expressed as means ± SEM. (a) black bars = untreated; green bars = 1 ng/ml eNAMPT-WT; grey bars = 5 ng/ml eNAMPT-WT; (b) black bars = untreated; grey bars = 1 ng/ml eNAMPT-monomer; (c) black bars = no inhibitor; purple bars = SB203580; grey bars = SB203580; blue bars = SP600125, brown bars = BAY 11-7082 Panel a and b: *P<0.05, **P<0.01, ***P<0.001; Panel c: : *P<0.05, **P<0.01 (SP600125); †P<0.05, ††P<0.01 (SP600125) by 2-way ANOVA with Sidak's post-test.

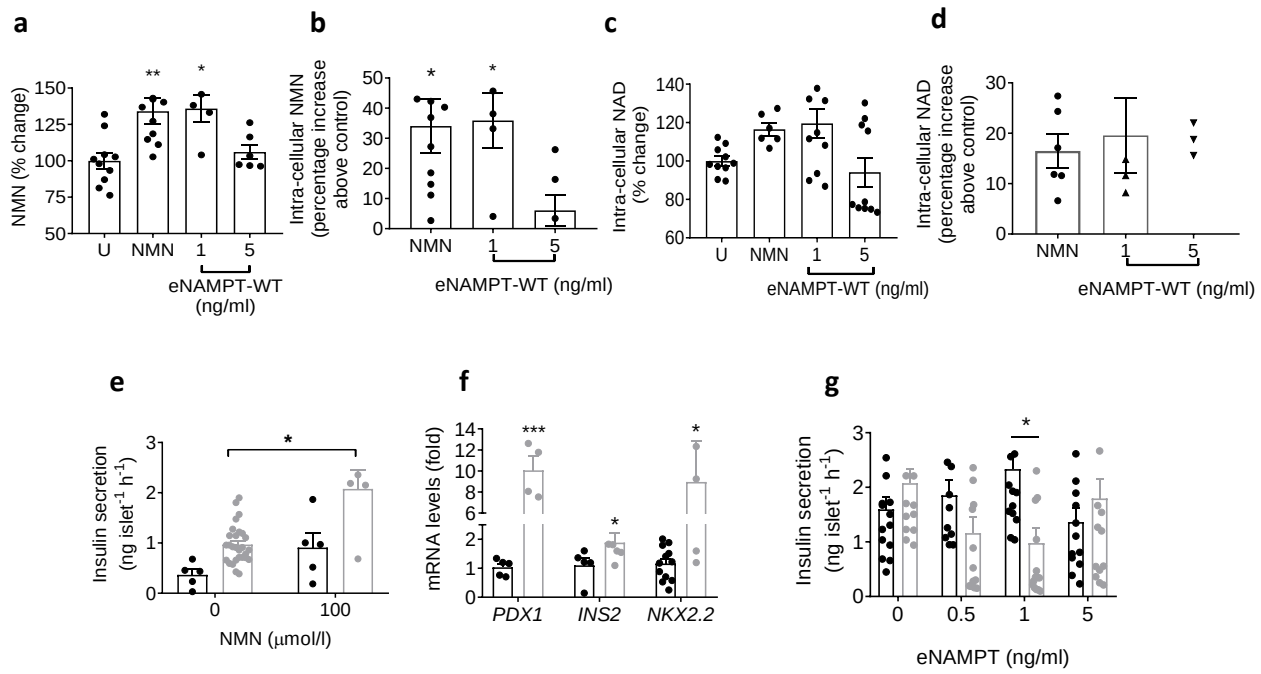

Figure 5: Structure-function changes mediate the bi-modal effects of eNAMPT-WT (a - d) MIN6 cells were incubated with either NMN (100 μmol/l) or eNAMPT-WT (1 – 5 ng/ml) for 48 h; **(a – b)** intra-cellular NMN, **(c –d)** intra-cellular NAD (*n*=5 -10, where n of 1 = 1 well of a 12 well plate). **(e-f)** Mouse islets were treated with NMN (100 μmol/l) **(E)** Static insulin secretion in response to 2 and 20 mmol/l glucose (n=5); **(f)** Gene expression levels of *PDX1*, *INS2* and *NKX2.2* measured by qPCR (*n*=5-12). **(g)** Mouse islets were treated for 48 h with eNAMPT-WT (0.5 – 5 ng/ml) in combination with the CD73 inhibitor AMCP, and static insulin secretion was measured in response to 20mM glucose (*n*=17). (f-g) black bars = untreated; grey bars = NMN. Data are expressed as means ± SEM, *P<0.05, **P<0.01, ***P<0.001, by 1- and 2-way ANOVA with Tukey's or Sidak's post-test.

ESM Methods

Human samples

Human serum samples were obtained from obese non-diabetic individuals (BMI: 46.4 +/- 1.8 kg/m^2; FPG: <5.6 mmol/L; Age: 53.0 +/- 2.0 years; n=13) and obese individuals with IFG (BMI: 37.5 +/- 1.9 kg/m^2; FPG 5.6 – 6.9 mmol/L; Age: 54.9 +/- 3.3 years; n=15) and type 2 diabetes (BMI: 36.3 +/- 1.6 kg/m^2; FPG ≥7.0 mmol/L; Age: 41.5 +/- 3.5 years; n=27), as part of the Body Fat, Surgery and Hormone study (BodyFatS&H) conducted at the University of Auckland, New Zealand (NTX/08/10/103; Northern Regional Ethics Committee, Auckland, New Zealand) and as part of the VaSera trial [1], conducted at St Thomas' Hospital, London (ISRCTN25003627; NRES Committee-London Central, 21/12/2012, ref: 12/LO/1850). VaSera trial participants consisted of individuals with type 2 diabetes or those at risk of developing type 2 diabetes (FPG: 5.6 – 6.9 mmol/L; BMI >30 kg/m^2).

Native Mass Spectrometry

The protein was expressed and isolated as previously described and, on the day of analysis, the buffer was exchanged into 100 mM ammonium acetate (Fisher Scientific, Loughborough, UK) pH 6.9 using micro Bio-Spin Chromatography columns (Bio-Rad, Micro Bio-Spin 6 Columns) following the instructions specified by the manufacturer. The procedure was repeated twice and diluted to give a final concentration of WT NAMPT (5 μmol/l) or S200D NAMPT (5 μmol/l). Native MS data was acquired on the Synapt G2S HDMS (Waters, Manchester, UK). NanoESI capillaries were prepared in-house from thin-walled borosilicate capillaries (inner diameter 0.9 mm, outer diameter 1.2 mm, World Precision Instruments, Stevenage, UK) using a Flaming/Brown P-1000 micropipette puller (Sutter Instrument Company, Novato, CA, USA). A positive voltage was applied to the solution via a platinum wire (Goodfellow Cambridge Ldt, Huntington, UK) inserted into the capillary. Gentle source conditions were applied to preserve the native-like structure: capillary voltage 1.2-1.5 kV, sampling cone 50-200 V, source temperature 70 °C. Trap collision energy was 4 V, transfer collsion energy was set to 0 V. Nitrogen was the carrier gas. External calibration of the spectra was achieved using solutions of cesium iodide (2 mg/mL in 50:50 water:isopropanol). Data were acquired and processed with MassLynx software (Waters, Manchester, UK).

eNAMPT protein generation

Construction of DNA plasmids: DNA for full length mouse NAMPT was synthesised as a double stranded DNA gBlock (Integrated DNA Technologies) and cloned into pET151 according to manufacturer's instructions (ThermoFisher). This vector adds an N-terminal 6xHis and V5 tag, and a TEV cleavage site, giving an extra 33 amino acids on the N-terminus of the protein. Mutagenesis was carried out to change residues S^{199} and S^{200} to D^{199} and D^{200} using the overlapping primers GGTTACAGAGGAGTCGACGATCAAGAGACTGCTGGC and GCCAGCAGTCTCTTGATCGTCGACTCCTCTGTAACC, and the Quikchange lightning kit (Agilent Technologies) according to the manufacturer's instructions. The constructs and mutations were verified by sequencing (Eurofins Genomics).

Expression of NAMPT wild type and eNAMPT-monomer (SS199/200DD) mutation: For expression, the constructs were transformed into BL21 Star (DE3) *E. coli* (ThermoFisher). Colonies were used to inoculate a starter culture in Luria Broth containing 100ug/mL ampicillin, and left shaking at 37^{o}C for 5 hours. This was used to inoculate 200mL ZYP-5052 autoinduction media (Studier, 2005) and the culture grown at 18^{o}C shaking for 65 hours. The bacteria were harvested by centrifugation at 4000g and frozen at -80^{o}C.

Purification of eNAMPT-WT and eNAMPT-WT (SSDD) mutation: Pellets were thawed and EDTA Complete protease inhibitor tablets added (Roche) then the *E. coli* were lysed using BugBuster (Merck Millipore, Burlington, MA, USA) according to the manufacturer's instructions. The NAMPT was found in the soluble fraction and was purified by passing over a 1mL Histrap ff crude column (GE Healthcare, Chicago, IL, USA) using a Biorad NGC system. The column was washed with 30 column volumes of 10mM sodium phosphate, 500 mmol/l NaCl, 20 mmol/l imidazole pH 7.4 and the bound protein eluted with 10 mmol/l sodium phosphate, 500 mmol/l NaCl, 500 mmol/l imidazole pH 7.4. Fractions containing protein were then pooled and concentrated (Amicon Ultra 15, Merck Millipore), then further purified using size exclusion chromatography. Using a Gilson HPLC system, samples were run on a Superdex 200 increase 10/300 GL column in Phosphate buffered saline pH 7.4 (OXOID). Fractions corresponding to monomer and dimer were pooled individually. Final yield of protein was approximately 40mg/L for the WT, 8mg/L for monomer SSDD fraction and 5mg/L dimer SSDD fraction.

Pancreatic islet isolation

Mouse CD1 Islets were isolated as described previously [2]. Pancreata were inflated with 1mg/mL collagenase solution (Sigma-Aldrich, Poole, U.K.) followed by density gradient separation

(Histopaque-1077; Sigma-Aldrich). Human islets were isolated from heart-beating non-diabetic donors, with appropriate ethical approval, at the King's College Hospital Human Islet Isolation Unit [2]. Isolated islets were incubated overnight (37°C, 5% CO_2) prior to treatments. See human islet checklist table for additional details of human islet preparations.

Static and dynamic glucose-stimulated insulin secretion

For static insulin secretion, mouse CD1 or human islets were pre-incubated in a physiological salt solution [3] containing 2mM glucose. Groups of 3-5 size-matched islets were then further incubated at 37°C for 1 h in salt solution and 2 or 20 mmol/l glucose. Dynamic insulin secretion was measured using a temperature-controlled perifusion system. Mouse CD1 islets were transferred into chambers containing 1 μm pore-size nylon filters (40 islets/chamber) and perifused with a physiological salt solution [3] (37°C, 0.5mL/min) containing 2 or 20 mmol/l glucose or 20 mmol/l glucose and 20 mmol/l KCl. Samples were collected at 2-minute intervals throughout the experiment. Secreted insulin was measured using an in-house I^{125} radioimmunoassay [3].

Quantitative RT-PCR

Total mouse CD1 or human islet RNA was extracted using Trizol reagent (Invitrogen, Paisley, UK). Reverse transcription was performed using the High-Capacity cDNA reverse transcription kit (Applied Biosystems, Warrington, UK). Real-time qPCR was carried out with a LightCycler480, using Sybr Green PCR master mix (Qiagen, Hilden, Germany). Gene expression was measured by ΔΔCt methodology, normalised against GAPDH (Quantitech, UK). For primer details (all Eurogentec, Southampton, UK) see ESM Table 1.

NMN measurements

NMN was measured in MIN6 cells and human serum using a fluorometric assay based on previous described methodology [4,5]. MIN6 or serum samples (30 μL) were extracted with 100 μL perchloric acid (1 mol/L) and then neutralized by addition of 330 μL K_2CO_3 (3 mol/L) followed by incubation at 4°C for 10 min, and centrifugation at 12000 x g for 15 min at 4°C, with the supernatant retained. Serum and cellular samples (50 μL) and standard solutions of NMN (50 μl; 25 – 200 μmol/l) were subsequently derivatised by addition of 20 μl KOH (1 mol/L) and 20 μl acetophenone (Sigma, Poole, UK) followed by incubation at 4°C for 15 min. Formic acid (90 μL) was then added and the solution incubated for 10 min at 37°C, producing a highly fluorescent compound. Samples or standards (150 μL) were then added into a 96-well plate fluorescence was detected on a SpectraMax i3x plate reader with excitation and emission wavelength of 382 and 445 nm, respectively.

eNAMPT Immunoblotting

Serum non-reducing immunoblotting was conducted as previously described. Primary antibody against NAMPT (both Cell Signaling Technologies, MA, USA) was used in this study (all primary antibodies were rabbit anti-mouse polyclonal and were used at 1:1000 dilutions). Immunoblots were conducted under non-reducing conditions, where no reducing agent was added to the protein samples prior to SDS-PAGE. This allows detection of both monomeric and dimeric eNAMPT in biological samples. Densitometry of western blot bands was calculated using Image J Software and densitometry data was used to calculate percentage ratio of eNAMPT monomer:dimer in ND and T2D serum. Concentrations of monomer and dimer in T2D serum were calculated by taking the total eNAMPT concentration present in the sample (as calculated by ELISA) and using the percentages derived from densitometry to calculate final serum concentrations of monomer and dimer. Western blots are representative of 3 separate blots. sTo ensure equivalent loading of each gel lane, serum protein was equalized to 10 μg and an equal volume (30 μl) was added to each well.

References

1. Mills CE, Govoni V, Faconti L, Casagrande ML, Morant SV, Webb AJ, et al. Reducing Arterial Stiffness Independently of Blood Pressure: The VaSera Trial. Journal of the American College of Cardiology. 2017;70(13):1683-4.

2. Huang GC, Zhao M, Jones P, Persaud S, Ramracheya R, Lobner K, et al. The development of new density gradient media for purifying human islets and islet-quality assessments. Transplantation. 2004;77(1):143-5.

3. Jones PM, Salmon DM, Howell SL. Protein phosphorylation in electrically permeabilized islets of Langerhans. Effects of Ca2+, cyclic AMP, a phorbol ester and noradrenaline. The Biochemical journal. 1988;254(2):397-403.

4. Formentini L, Moroni F, Chiarugi A. Detection and pharmacological modulation of nicotinamide mononucleotide (NMN) in vitro and in vivo. Biochemical pharmacology. 2009;77(10):1612-20.

5. Zhang RY, Qin Y, Lv XQ, Wang P, Xu TY, Zhang L, et al. A fluorometric assay for high-throughput screening targeting nicotinamide phosphoribosyltransferase. Analytical biochemistry. 2011;412(1):18-25.

ESM Table 1

Primers for qPCR

Human primers

Gene	Forward primer (5'-3')	Reverse primer (3'-5')
IL1β	GGCTGCTCTGGGATTCTCTT	CCATCATTTCACTGGCGAGC
CCL2	CACCTGGACAAGCAAACCCA	GTGTCTGGGGAAAGCTAGGG
TNFα	GCCCATGTTGTAGCAAACCC	TATCTCTCAGCTCCACGCCA

Mouse primers

Gene	Forward primer (5'-3')	Reverse primer (3'-5')
GAPDH	AGGGCTGCTTTTAACTCTGGT	CCCCACTTGATTTTGGAGGGA
PDX1	GAACCCGAGGAAAACAAGAGG	GTTCAACATCACTGCCAGCTC
INS2	CCGTGGTGAAGTGGAGGA	CAGTTGGTAGAGGGAGCAGAT
NKX2.2	CCTTTCTACGACAGCAGCGA	CCGTGCAGCGAGTATTGCAG
NKX6.1	CAAGGCTGCACATCGTGTTT	GAACAGGCTAGGTGGGTCTG
Il1B	GGGCTGCTTCCAAACCTTTG	TGATACTGCCTGCCTGAAGCTC
CCL2	GGCTGGAGAGCTACAAGAGG	GGTCAGCACAGACCTCTCTG
TNFA	CGGAGTCCGGGCAGGT	GCTGGGTAGAGAATGGATGAACA

ESM Table 1. Table of mouse and human qPCR primers

ESM Figures

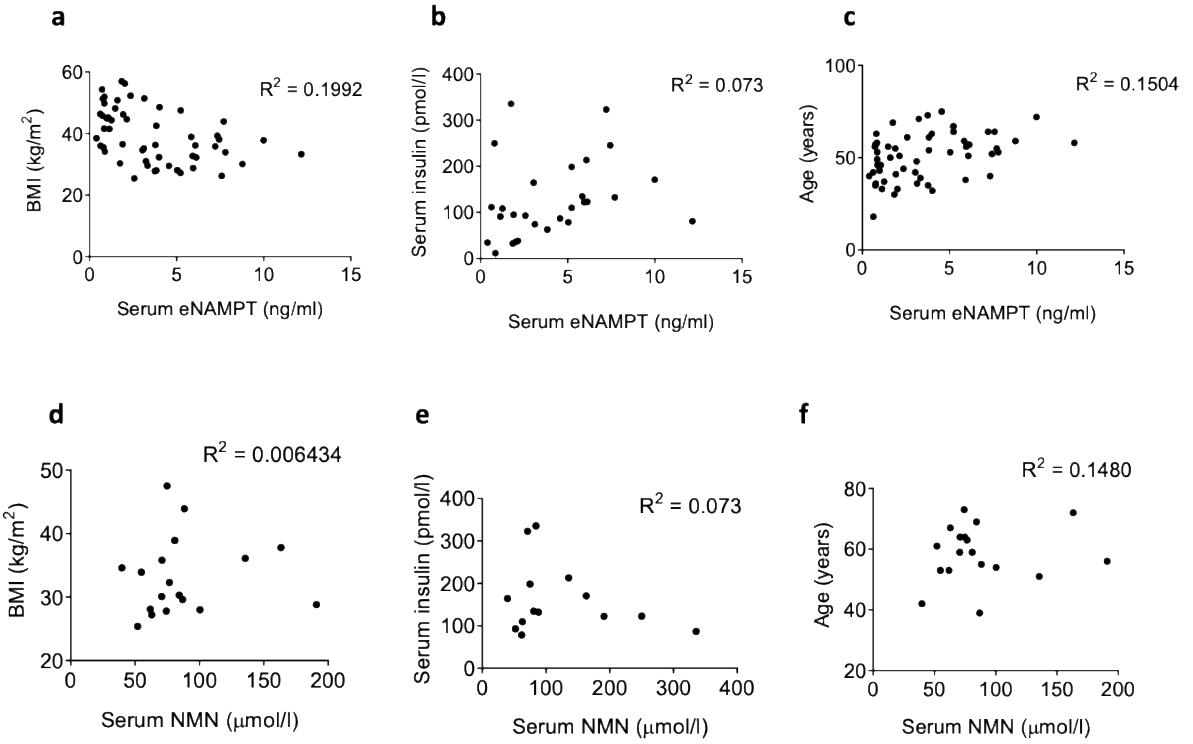

ESM Figure 1: Serum eNAMPT and NMN levels are not correlated with BMI or age. Serum was collected from non-diabetic, IFG and type 2 diabetic individuals, and eNAMPT and NMN were measured by ELISA and fluorometric assay, respectively**. (a)** Serum eNAMPT vs BMI (data generated from BodyFatS&H and VaSera trial samples); **(b)** Serum NMN vs serum insulin; **(c)** Serum eNAMPT vs. age (data generated from BodyFatS&H and VaSera trials). **(d)** Serum NMN vs BMI (data generated from BodyFatS&H and VaSera trial samples); **(e)** Serum NMN vs serum insulin; **(f)** Serum NMN vs age (NMN data generated from VaSera trial only). N is equal to 1 individual. N values differ for NMN measurements due to limited sample availability for some samples. Statistics were calculated using Pearson correlation.

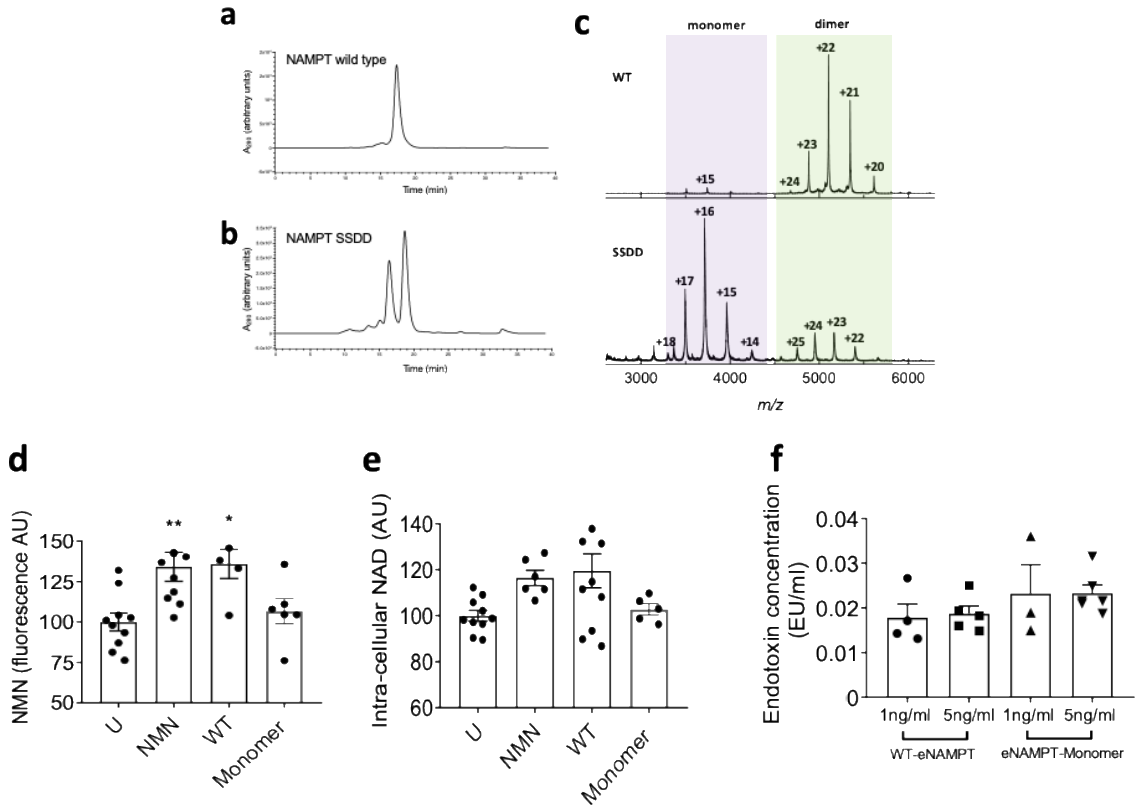

ESM Figure 2: Structural and functional characterisation of eNAMPT-monomer and eNAMPT-WT. (a-b) Size exclusion chromatography data showing **(a)** eNAMPT-WT and **(b)** eNAMPT-monomer (SSDD); **(c)** Native mass spectra of 6.5 μM eNAMPT-WT and 5 μM eNAMPT-monomer (SSDD) in 100 mM ammonium acetate showing differences in the monomer to dimer distribution. **(D – E)** MIN6 cells were incubated with either NMN (100 μM), WT-eNAMPT (1 ng/mL) or eNAMPT-monomer (1 ng/mL) for 48 hours; (**d)** intra-cellular NMN, **(e)** intra-cellular NAD (*n*=5 – 10). **(f)** Endotoxin concentrations in preparations of WT-eNAMPT and eNAMPT-monomer. Data are expressed as means ± SEM. *P<0.05, **P<0.01 by 1-way ANOVA followed by Tukey's post-test

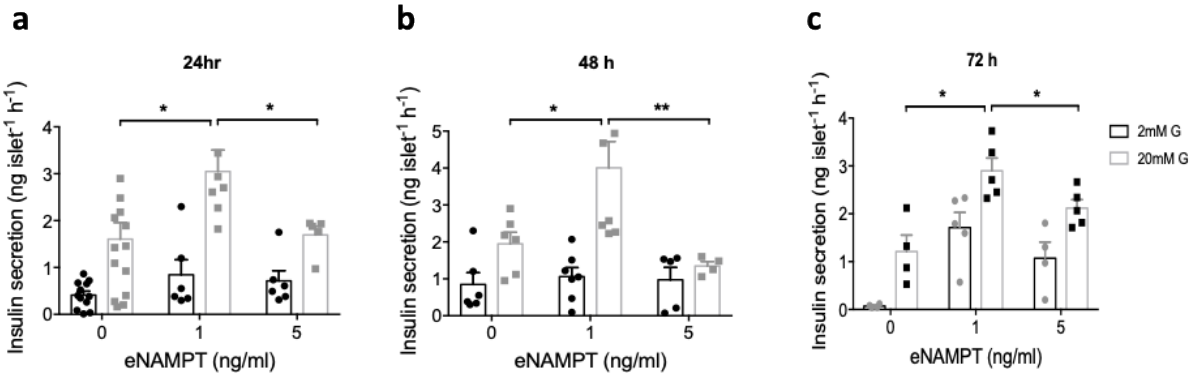

ESM Figure 3: Commercially obtained eNAMPT exerts a bi-phasic effect on glucose-stimulated insulin secretion Static insulin secretion in response to basal (2mM) or 20mM glucose was assessed in isolated mouse islets incubated with 1 – 5 ng/mL commercially obtained eNAMPT (Adipogen, Seoul, South Korea) for **(a)** 24 hours *(n*=12), **(b)** 48 hours *(n*=6) and **(c)** 72 hours *(n*=5). Data are expressed as mean ± SEM, *P<0.05, **P<0.01, by 2-way ANOVA followed by Sidak's post-test.

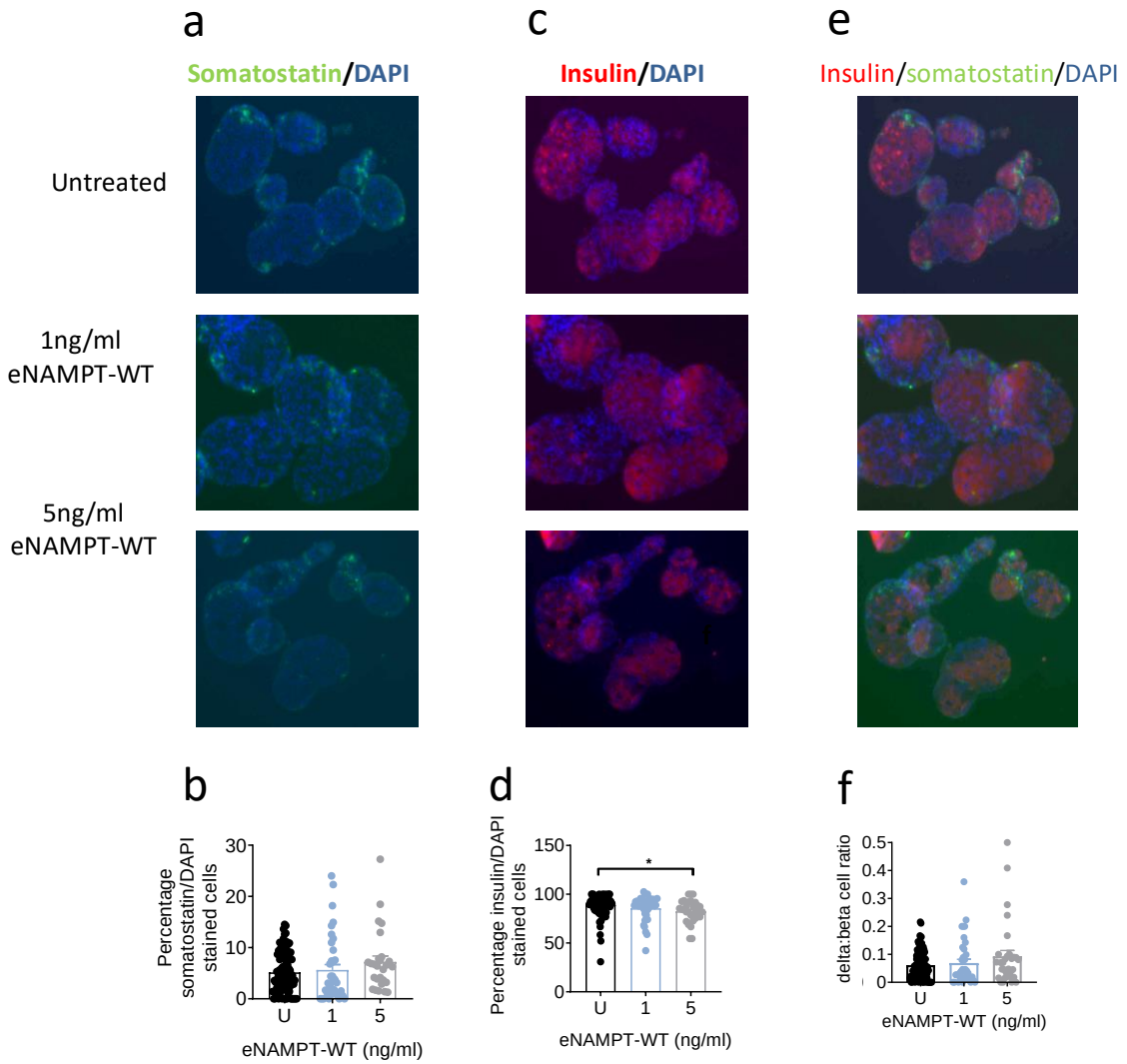

ESM Figure 4: Effects of eNAMPT-WT on islet delta-cell number. Mouse islets were treated with 1 – 5 ng/mL eNAMPT-WT for 48 h **(a)** Double immunofluorescence images of islets stained for somatostatin (green) and DAPI (blue) **(b)** % DAPI/SST positive stained cells *(n*=3); **(c)** Double immunofluorescence images of islets stained for insulin (red) and DAPI (blue) **(d)** % DAPI/INS positive stained cells *(n*=3); (**e)** Immunofluorescence images of islets stained for SST (green), INS (red) and DAPI (blue) **(f)** % DAPI/SST:% DAPI/INS stained cells *(n*=3); Data are expressed as means ± SEM, *P<0.05, by 1-way ANOVA with Tukey's post-test.

Checklist for reporting human islet preparations used in research

Adapted from Hart NJ, Powers AC (2018) Progress, challenges, and suggestions for using human islets to understand islet biology and human diabetes. Diabetologia https://doi.org/10.1007/s00125-018-4772-2

Islet preparation	1	2	3	4	5
MANDATORY INFORMATION					

Unique identifier	Unknown	Unknown	Unknown	Unknown	Unknown
Donor age (years)	50	49	26	49	59
Donor sex (M/F)	Male	Male	Male	Female	Female
Donor BMI (kg/m^2)	Unknown	Unknown	Unknown	Unknown	24
Donor HbA_{1c} or other measure of blood glucose control	Unknown	Unknown	Unknown	Unknown	Unknown
Origin/source of islets[b]	King's College Hospital islet transplantation unit	King's College Hospital islet transplantation unit	King's College Hospital islet transplantation unit	King's College Hospital islet transplantation unit	King's College Hospital islet transplantation unit
Islet isolation centre	King's College Hospital islet transplantation unit	King's College Hospital islet transplantation unit	King's College Hospital islet transplantation unit	King's College Hospital islet transplantation unit	King's College Hospital islet transplantation unit
Donor history of diabetes? Please select yes/no from drop down list	No	No	No	No	No
Diabetes duration (years)	N/A	N/A	N/A	N/A	N/A
Glucose-lowering therapy at time of death[c]	N/A	N/A	N/A	N/A	N/A
RECOMMENDED INFORMATION					
Donor cause of death	Unknown	Donation after brain death	Donation after circulatory death	Unknown	Unknown
Warm ischaemia time (h)	Unknown	Unknown	Unknown	Unknown	Unknown
Cold ischaemia time (h)	Unknown	Unknown	Unknown	Unknown	Unknown
Estimated purity (%)	75-80	55	80	70	Unknown
Estimated viability (%)	85	80	80	80	Unknown
Total culture time (h)[d]	72 hours	72 hours	72 hours	120 hours	72 hours
Glucose-stimulated insulin secretion or other functional measurement[e]	Glucose-stimulated Insulin secretion and RNA extraction for qPCR	RNA extraction for qPCR	Glucose-stimulated Insulin secretion	Glucose-stimulated Insulin secretion and RNA extraction for qPCR	Glucose-stimulated Insulin secretion
Handpicked to purity? Please select yes/no from drop down list	Yes	Yes	Yes	Yes	Yes
Additional notes					

[a]If you have used more than eight islet preparations, please complete additional forms as necessary
[b]For example, IIDP, ECIT, Alberta IsletCore
[c]Please specify the therapy/therapies
[d]Time of islet culture at the isolation centre, during shipment and at the receiving laboratory
[e]Please specify the test and the results